PAPER

Check for updates

Microscopic vibrational circular dichroism on the forewings of a European hornet: heterogenous sequences of protein domains with different secondary structures†

Hisako Sato, [ID] *[a] Sayako Inoué,[b] Jun Yoshida, [ID] [c] Izuru Kawamura,[d] Jun Koshoubu[e] and Akihiko Yamagishi[f]

We developed a microscopic scanning for vibrational circular dichroism (VCD) spectroscopy in which a quantum cascade laser is equipped with a highly focused infrared light source to attain a spatial resolution of 100 μm. This system was applied to the forewing of a European hornet to reveal how the protein domains are organised. Two-dimensional patterns were obtained from the VCD signals with steps of 100 μm. We scanned the 1500–1740 cm^{-1} wavenumber range, which covers amide I and II absorptions. Zone sequenced α-helical and β-sheet domains within an area of 200 μm^2 in membranes close to where two veins cross. The sign of the VCD signal at 1650 cm^{-1} changed from positive to negative when probed along the zone axis, intermediated by the absence of VCD activity. The significance of this zone is discussed from the viewpoint of the mechanical properties required for flying motion. These features are unattainable using conventional FTIR (Fourier transform infrared) or FT-VCD methods with a spatial resolution of ~10 mm^2.

Introduction

Recently, several attempts have been made to augment chiroptical spectroscopies with scanning functions.[1–7] In the case of vibrational circular dichroism (VCD), microscopic scanning is useful for heterogeneous samples that exhibit supramolecular chirality.[3] For example, VCD using a quantum cascade laser as an IR source (QCL-VCD) has been used to study the chiral properties of amyloid-like tissues.[5,6]

Recently, we reported the construction of a QCL-VCD system capable of microscopic scanning,[8–11] in which VCD signals are collected along multiple axes (wavenumber, positional coordinate, and time). A two-dimensional VCD signal pattern was

obtained at a spatial resolution of 100 μm.[10] The developed instrument is referred to as the "multi-dimensional VCD" (MultiD-VCD) system. The system was applied to the *in situ* analysis of the hindwings of a beetle,[11] which revealed that the hindwings comprise segregated microdomains of proteins with different secondary structures, with coil/PPII (polyproline II) and α-helix structures determined to dominate in the veins and membranes, respectively. More recently, the investigation was extended to other species, such as beetles, European hornets, and dragonflies.[12] For example, the β-sheet domain dominates the membranes of a European hornet, while no VCD activity is observed for a dragonfly. These results suggested that the structure of the protein domain may reflect the flying type.

The next problem involves determining how the protein domains in different secondary structures are organised to realise the mechanical properties needed for flying motion.[12–29] As far as our literature survey is concerned, the issue remains unclear despite intensive spectroscopic investigations.[13–33] Some studies have suggested that resilin plays a role as a flexible adhesive in veins.[29–36]

Herein, we used MultiD-VCD to study the forewings of *Vespa crabro flavofasciata* Cameron, 1903. This revealed that a belt zone with α-helix and β-sheet sequenced domains exists within an area of 200 μm^2 in size at boundary regions where veins and membrane cross. Hybridising the protein domains in different structures is important for realising the mechanical properties required for flying. These features are unattainable when the

^{a} *Faculty of Science, Ehime University, 1 2-5, Bunkyo-cho, Matsuyama, 790-8577, Japan. E-mail: sato.hisako.yq@ehime-u.ac.jp*

^{b} *Geodynamics Research Center, Ehime University, Matsuyama 790-8577, Japan*

^{c} *Department of Chemistry, College of Humanities & Sciences, Nihon University, Setagaya-ku, Tokyo 156-8550, Japan*

^{d} *Graduate School of Engineering Science, Yokohama National University Yokohama, 240-8501, Japan*

^{e} *JASCO Corporation, Ishikawa 2967-5, Hachioji Tokyo, 192-8537, Japan*

^{f} *Faculty of Medicine, Toho University, 2 5-21-16 Oomori-nishi, Ota-ku, Tokyo, 143-8540, Japan*

† Electronic supplementary information (ESI) available: Optical microscopy; polarized light microscopy; detailed IR and VCD mapping data; IR and VCD maps of dorsal and ventral surfaces; IR and VCD spectra of a left forewing. See DOI: https://doi.org/10.1039/d4cp01827c

17918 | *Phys. Chem. Chem. Phys.*, 2024, 26, 17918–17922

This journal is © the Owner Societies 2024

acquired VCD signals are averaged over an area of ~ 10 mm^2 using conventional FT-IR or FT-VCD spectroscopies.

Results and discussion

Samples and focus points

A hornet, *Vespa crabro flavofasciata* (female), was selected as the sample. This insect is an endangered species and it has four wings: two forewings and two hind wings. Fig. S1(a) and (b) (ESI†) show the left and right forewings (dorsal) of a European hornet acquired by optical microscopy (ESI†). Each wing consists of a vein network (costa, cubitus radius, medial and anal vein) and membranes.[30] The present study observed a forewing, focusing on the membrane region close to where two veins intersect.

The main role of the wing is to generate dynamic lift for flight. This motion is accompanied by wing deformation, such as curving; consequently, flexibility is required for the wing to achieve its curve design. However, acquiring such mechanical properties using the uniform composition of a single protein structure is challenging. Domains containing resilin are reportedly present within veins.[30] Resilin is characterised by rubber-like elasticity that reduces stress. Obtaining evidence that connects protein domains in different secondary structures is an interesting objective.[29]

Scanning electron microscopy and polarised light microscopy

Fig. 1 shows scanning electron microscopy (SEM) images of the dorsal and ventral surfaces of the right forewing. The observed areas are located at the crossing-vein/membrane boundaries. Veins have compartment-like structures and are about 50-μm-thick, while the membrane surfaces are covered with microtrichia.

Fig. S2(left) (ESI†) shows a polarised light microscope image of the left forewing (ESI†). A two-vein crossing region is observed on the ventral side of the wing. The vein is estimated to be 65-μm wide. Dark belts are observed on both sides of each vein which are optically isotropic and non-crystalline. Bright

regions are observed along the veins, which indicates that they are oriented and show dichroic effects. The same area of the right forewing was also observed by microscopy (Fig. S2(right)) (ESI†). No significant differences were observed between the left and right forewings.

Microscopic IR and VCD measurements

The light-brown right hindwing of the hornet was sandwiched between two CaF$_2$ substrates in a cell (17 mm diameter). The wing was estimated to be 7–10 μm thick. Fig. 2(b) and (c) show IR and VCD maps of the right forewing acquired at 1650 cm^{-1} in 0.25 mm steps, respectively. The ventral wing was scanned. The IR wavenumber corresponds to the amide I band of proteins, which confirmed that proteins are present in measurable amounts over the entire scanned area. The VCD map shows both positive and negative signs, which indicates that more than two protein domains with different secondary structures coexist.

Fig. 3(a) shows IR and VCD spectra acquired for the membrane near the point where two veins intersect. Four positions were selected, as indicated by the green, blue, red, and black circles (Fig. 3(b)). Notably, the VCD spectra were found to be dramatically position-dependent, which indicates that the protein structure varies within an area as small as 200 μm^2. However, the IR spectra remained almost the same. Positive and negative peaks were observed at 1650 and 1630 cm^{-1} in the green circle with reversed signs observed in the red circle. The VCD spectrum acquired in the blue circle was weak; however, it recovered in the black circle. These results indicate the existence of a sequence of protein domains with different secondary structures along the vertical direction (indicated by the black arrow in Fig. 2(b)).

The secondary structure of the protein at each circle was identified by comparing the obtained VCD spectra with those reported for authentic samples of various secondary strucutures.[37–48] From this comparison, we deduced that the domains change from β-sheet (green circle) to α-helix (red circle), and then return to β-sheets (black circle) (Fig. 3(c)). The VCD
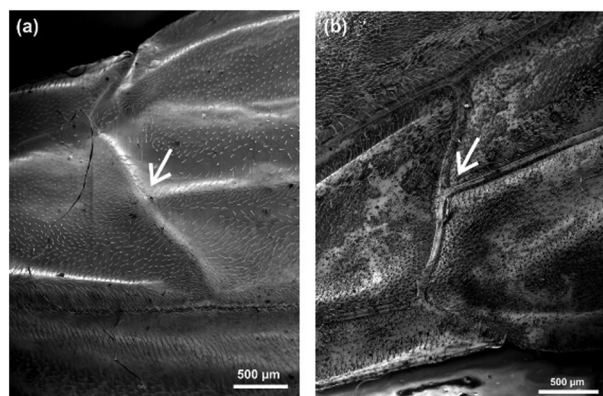

Fig. 1 SEM images of the (a) dorsal and (b) ventral surfaces of a right forewing. Arrows indicate the crossing points of two veins. The same arrows are indicated in the IR map shown in Fig. 2.
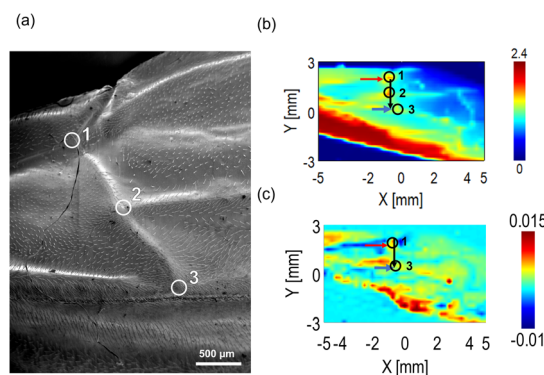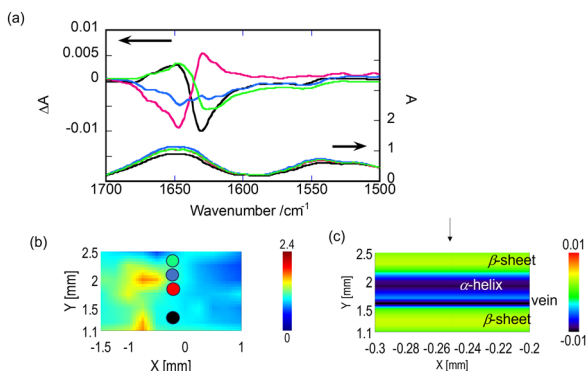

Fig. 2 (a) SEM image showing the correspondence between IR and VCD maps and wing topology in Fig. 1(a). The highlighted open circles indicated as 1, 2 and 3 correspond to the vein-crossing regions as seen in (b) and (c). (b) and (c) Two-dimensional (b) IR and (c) VCD maps of a right forewing acquired at 1650 cm^{-1}. The black, red, and blue arrows in panel (b) indicate microscopic measurement directions (see text).

This journal is © the Owner Societies 2024

Phys. Chem. Chem. Phys., 2024, **26**, 17918–17922 | **17919**

Fig. 3 (a) IR (lower) and VCD (upper) spectra for selected points along the black arrow (Fig. 2(b)) of the right forewing, as indicated by the circles (black, red, blue, and green) in panel (b). (b) Coordinates of the selected circles: black (-0.25, 1.2), red (-0.25, 1.9), blue (-0.25, 2.1), and green (-0.25, 2.3). (c) Secondary structures are sequentially assigned in the Y-direction as: β-sheet, low intensity VCD (proposed to be PPII), α-helix, and vein region. The VCD map acquired at 1648 cm^{-1} is shown. The measured points move in the direction of the arrow in 0.1 mm steps.

spectrum acquired in the blue circle was almost flat, as indicated by the blue line in Fig. 3(a).

There are two possible explanations for the low VCD activity observed in the blue circle. One involves the overlap of positive (α-helix) and negative (β-sheet) signals at 1630 cm^{-1}, while the two domains are affected by a region of low VCD activity in the other. The latter possibility is of interest if a resilin domain is present between the two domains. Resilin is reported to have no unique secondary structure, such as hydrogen-bonded β-sheets or α-helices.[29] Instead, its conformation depends on the stress conditions: PPII in its stretched state and β-turns in its compressed state. Keiderling *et al.* reported the VCD signal for protein and peptide various authentic secondary structures. A PPII helical structure was included. In the present work, the signal for the intermediate region was similar to that reported to the PPII structure.[39,48] No VCD signal enhancement is observed in cases where proteins lack stereoregular ordering over a few hundred nanometres.[49] Thus, they are seemingly VCD inactive. The corresponding details are discussed in a subsequent section.

Fig. S3 (ESI†) shows the results of more detailed measurements along the black arrow in Fig. 2(b), which were intended to provide more accurate VCD spectra during the transition from positive to negative sign (ESI†). VCD signal reversal was confirmed when the probe was moved downward along the arrow. The VCD spectrum at the transition point of sign reversal is similar to that reported for PPII structures;[39] however, it was similar to the difference between the two spectra before and after signal change. Consequently, no definite conclusion can be drawn as to which of the above possibilities is more plausible. Therefore, determining whether resilin domains are present in the investigated region is necessary.

We acquired additional microscopic VCD data by probing in the horizontal direction, as indicated by the red arrow in Fig. 2(b), the results of which are shown in Fig. S4 (ESI†). Note

that the VCD signal changed in this direction. Consequently, we believe that a heterogeneous sequence exists widely at the boundary regions between veins and membranes. These results were obtained for the ventral side of the forewing.

For comparison, the dorsal side of the same sample was subjected to VCD scanning, with almost identical results obtained (Fig. S5 and S6) (ESI†). Therefore, the observed heterogeneous sequence is not restricted to the surface region but exists throughout the inner part of the wing.

For comparison, microscopic IR and VCD data were acquired at three positions near the vein, as indicated by the blue arrow in Fig. 2(b). The selected positions are shown in Fig. 4(a) and (b). Unlike the results shown in Fig. 3, the spectra are almost identical, with positive and negative peaks observed at 1660 and 1630 cm^{-1}, respectively. In addition, a small shoulder was observed at around 1680 cm^{-1}. We conclude that this region uniformly comprises β-sheet and β-turn protein hybrids, consistent with previous reports.[12]

Similar microscopic IR and VCD data were acquired for the corresponding regions of the left forewing. Fig. S7 (ESI†) shows that a heterogeneous sequence of protein domains was observed in a similar manner as observed for the right wing (ESI†). These results suggest that these regions play the same roles in both the right and left wings.

Functional significance of heterogeneously linked protein domains

The microscopic VCD data revealed that the protein structure changes sequentially in the membrane region close to where two veins intersect; this change occurs within an area as small as 200 μm^2. Moreover, there is an intermediate region that is VCD inactive. A suggested possibility involves the intervention of resilin domains between the α-helix and β-sheet regions.

The role of the observed heterogeneous sequence of protein domains may be rationalised by assuming that hybridising the two domain types provides a wing with appropriate elasticity and stiffness. In the case of a hornet, the forewings and hindwings are connected by hooks and move as a single organ.[29] Mechanical flexibility is proposed to be facilitated by the resilin domains in the veins. These residues ensure that the wings assume a folded form during curving while flying. Accordingly, the membrane region close to each vein may be stressed, requiring some flexibility consequently.
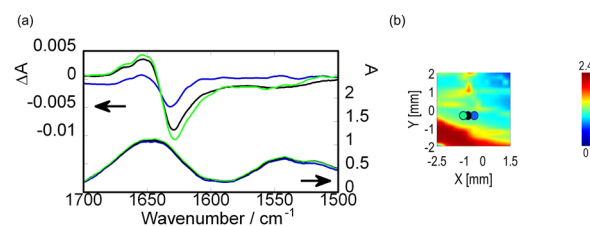
Fig. 4 (a) IR (lower) and VCD (upper) spectra acquired at the selected points along the blue arrow (Fig. 2(b)) of the right forewing, as indicated by circles (black, red, green, and blue) in panel (b). (b) Circle coordinates: green (-1.0, -0.5), black (-0.75, -0.5), and blue (-0.5, 0.5).

17920 | *Phys. Chem. Chem. Phys.*, 2024, **26**, 17918–17922

This journal is © the Owner Societies 2024

The anisotropy ($\Delta A/A$) values of the present samples were determined to be about 0.01. This value is much higher than those of typical VCD signals associated with single amino acid molecules ($\Delta A/A \sim 0.001$). In other words, this observation is realised through VCD signal enhancement associated with the formation of supramolecular chirality. According to our theoretical simulations, the VCD signal enhancement is observed for peptide chains with more than 100 amino acid residues that are stereoregularly linked.[49] Based on this prediction, randomly coiled proteins may be responsible for the VCD inactivity observed for the intermediate region between the α-helices and β-sheets.

Experimental

Insect wing sampling

Vespa crabro flavofasciata Cameron, 1903 (female) was sampled. European hornets are endangered and were donated by the Biodiversity Center of Ehime Prefectural Institute of Public Health and Environmental Science. Some *Vespa crabro flavofasciata* were caught in Imabari, Ehime, Japan; they were dead body samples. The forewing of the insects was sandwiched between two CaF_2 plates (17 mm diameter), as described in the Results and discussion section.

Polarised light microscopy

Polarised light microscopy images of the forewings were acquired using a polarising optical microscope (BX-53, Olympus Corp.).

Scanning electron microscopy (SEM)

Wing samples were coated with gold films using a JEOL JFC-1600 coater at a sputtering current of 20 mA for 60 s. SEM images were obtained using a field-emission scanning electron microscope (JEOL JSM-IT500HR) operating at 3 kV.

QCL-VCD

VCD spectra were acquired using an instrument developed in-house in cooperation with the JASCO Corporation, Japan. The instrument is referred to as the "MultiD-MIRAI-2020 spectrometer", and is a concurrent system augmented with QCL-VCD (quantum cascade laser) capabilities that cover the 1500-1740 cm^{-1} wavenumber range. The infrared light from a quantum cascade laser was focused using two BaF_2 plano-convex lenses. The spatial resolution was set to 100 μm. To avoid disturbance from water vapour, the cell compartment was purged with flowing dry N_2 from an M2NT-0.4II-6 N_2-gas generator (KOFLOC (Kyoto, Japan)) at approximately 6 L min^{-1}.[8,9]

The laser light source covered the wavenumber region associated with the amide groups of amino acids or peptides. In this study, we used the QCL-VCD method with an automatic microscopic scanning function.

The original mapping data were acquired when the sample was scanned using an automatic microsampling accessory with focusing lenses. At first, scanning was performed at a fixed wavenumber of 1650 cm^{-1} with an interval of 0.25 mm over an approximate 10 × 10 mm area, after which a smaller area was scanned in the 1500–1740 cm^{-1} range. During mapping, the sample stage was moved one or two-dimensionally with steps of 100 μm. Spectra were recorded in the 1500–1740 cm^{-1} wavenumber range while scanning in 1.0 cm^{-1} increments. IR and VCD signals were acquired only once. Less than 4s was required to acquire data at each wavenumber, and the baseline was not corrected. The data were processed by applying Savitzky–Golay smoothing with 13 points to reduce noise levels.

Conclusions

Insect wings were investigated using a multi-dimensional VCD system (MultiD-VCD) augmented with a quantum cascade laser, with forewing samples of European hornets (*Vespa crabro flavofasciata*) used. Two-dimensional VCD signal maps were created for membrane regions close to where veins cross. The VCD signal was observed to change dramatically within a narrow region less than 200 $μm^2$ in size. We conclude that the α-helical and β-sheet structural domains are connected. The observed heterogeneous connections may be necessary for the membrane to acquire elasticity and stiffness during flapping. The present work demonstrates the utility of MultiD-VCD in studying the organisation of protein structures based on signal enhancement in supramolecular chirality.

Author contributions

Hisako Sato (conceptualization, investigation, VCD methodology, and writing the original draft). Sayako Inoué, (SEM, data curation, writing the original draft, discussion). Jun Yoshida (polarized light microscopy, data curation). Izuru Kawamura (data curation, discussion). Jun Koshoubu (VCD instrument development). Akihiko Yamagishi (conceptualization, investigation, discussion, writing the original draft). All authors contributed equally.

Data availability

The data supporting this article have been included as part of the ESI† and the digital data of this study are available from the corresponding authors upon reasonable request.

Conflicts of interest

There are no conflicts to declare.

Acknowledgements

This journal is © the Owner Societies 2024

Phys. Chem. Chem. Phys., 2024, **26**, 17918–17922 | 17921

Usage/Research Centre of PRIUS (Project No. 2024-D01) at Ehime University, Japan.

Notes and references

1 G. Albano, A. Taddeucci, G. Pescitelli and L. D. Bari, *Chem. – Eur. J.*, 2023, **29**, e202301982.

2 L. A. Nafie, *Chirality*, 2020, **32**, 667.

3 X. Lu, H. Li, J. W. Nafie, T. Pazderka, M. Pazderková, R. K. Dukor and L. A. Nafie, *Appl. Spectrosc.*, 2017, **71**, 1117.

4 A. Kaczor, *Phys. Chem. Chem. Phys.*, 2023, **25**, 19371.

5 Y. Phal, K. Yeh and R. Bhargava, *Anal. Chem.*, 2021, **93**, 1224.

6 Y. Phal, L. Pfisrwe, P. Scott and R. Bhargava, *J. Phys. Chem. C*, 2022, **126**, 9777.

7 S. Lüdeke, M. Pfeifer and P. Fischer, *J. Am. Chem. Soc.*, 2011, **133**, 5704.

8 H. Sato, *Phys. Chem. Chem. Phys.*, 2020, **22**, 7671.

9 H. Sato, M. Shimizu, K. Watanabe, J. Yoshida, I. Kawamura and J. Koshoubu, *Anal. Chem.*, 2021, **93**, 2742.

10 H. Sato, M. Shimizu, K. Watanabe, J. Yoshida, I. Kawamura and J. Koshoubu, *Chem. Lett.*, 2021, **50**, 1543.

11 H. Sato, A. Yamagishi, M. Shimizu, K. Watanabe, J. Yoshida, I. Kawamura and J. Koshoubu, *J. Phys. Chem. Lett.*, 2021, **12**, 7733.

12 H. Sato, J. Koshoubu, S. Inoué, I. Kawamura and A. Yamagishi, *Chirality*, 2024, **36**, e23655.

13 J. Hasan, A. Roy, K. Chatterjee and P. D. D. V. Yarlagadda, *ACS Biomater. Sci. Eng.*, 2019, **5**, 3139.

14 S. H. Eraghi, A. Toofani, A. Khaheshi, M. Khorsandi, A. Darvizeh, S. Gorb and H. Rajabi, *Adv. Sci.*, 2021, **8**, 2004383.

15 P. Vukusic and J. R. Sambles, *Nature*, 2003, **424**, 852.

16 S. Müller, E. Garcia-Gonzalez, E. Genersch and R. D. Süssmuth, *Nat. Prod. Rep.*, 2015, **32**, 765.

17 J. Xiang, J. Du, D. Li and C. Zhen, *Microsc. Res. Tech.*, 2016, **79**, 550.

18 M. K. Salcedo and J. J. Socha, *Integr. Comp. Biol.*, 2020, **60**, 1208.

19 V. Sharma, M. Crne, J. O. Park and M. Srinvasarao, *Science*, 2009, **325**, 449.

20 F. Kaneko, C. Katagiri, G. Sazaki and K. Nagaghima, *J. Phys. Chem. B*, 2018, **122**, 12322.

21 S. Stuhr, V. K. Truong, J. Vongsvivut, T. Senkbeil, Y. Yang, M. A. Kobaisi, V. A. Baulin, M. Werner, S. Rubanov, M. J. Tobin, P. Cloetens, A. Rosenhahn, R. N. Lamb, P. Luque, R. Marchant and E. P. Ivanova, *Sci. Rep.*, 2018, **8**, 8413.

22 S. Eddy and T. Gullion, *J. Phys. Chem. C*, 2021, **125**, 931.

23 G. Qin, X. Hu, P. Cebe and D. L. Kapalan, *Nat. Commun.*, 2012, **3**, 1003.

24 G. Qin, S. Lapidot, K. Numata, X. Hu, S. Meirovitch, M. Dekel, I. Podoler, O. Shoseyov and D. L. Kaplan, *Biomacromolecules*, 2009, **10**, 3227.

25 G. Qin, S. Lapidot, K. Numata, X. Hu, S. Meirovitch, M. Dekel, I. Podoler, O. Shoseyov and D. L. Kaplan, *Biomacromolecules*, 2009, **10**, 3227.

26 S. Cheeseman, V. K. Truong, V. Walter, F. Thalmann, C. M. Marques, E. Hanssen, J. Vongsvivut, M. J. Tobin, V. A. Baulin, S. Juodkazis, S. Maclaughlin, G. Bryant, R. J. Crawford and E. P. Ivanova, *Langmuir*, 2019, **35**, 2422.

27 S. H. Nguyen, H. K. Webb, J. Hasan, M. J. Tobin, D. E. Mainwaring, P. J. Mahon, R. Marchant, R. J. Crawford and E. P. Ivanov, *Vib. Spectrosc.*, 2014, **75**, 173.

28 J. Goczał and R. G. Beutel, *Biol. Lett.*, 2023, **19**, 20220559.

29 E. Appel, J. Michels and S. N. Gorb, *Adv. Funct. Mater.*, 2023, **33**, 2215162; B. N. Danforth, *J. Zool.*, 1989, **218**, 247.

30 D. Hou and Z. Zhong, *Biomimetics*, 2023, **8**, 451.

31 S. Donoughe, J. D. Crall, R. A. Merz and S. A. Combes, *J. Morphol.*, 2011, **272**, 1409.

32 J. Sun and B. Bhushan, *C. R. Mec.*, 2012, **340**, 3.

33 J. Sun and B. Bhushan, *RSC Adv.*, 2012, **2**, 12606.

34 V. Machovič, L. Lapčák, M. Havelcová, L. Borecká, M. Novotná, M. Novotná, I. Javůrková, I. Langrová, Š. Hájková, A. Brožová and D. Titěra, *Sci. Agri. Bohemica*, 2017, **48**, 22.

35 L. Yu, J. Zhao, W. Wang, L. Zong, S. Ge and S. Yan, *Soft Matter*, 2023, **19**, 841.

36 F.-O. Lehmann, S. Gorb and B. Moussian, *Insect Biochem. Mol. Biol.*, 2024, **168**, 104089.

37 A. Kurochka, J. Pruůša, J. Kessler, J. Kapitán and P. Bouř, *Phys. Chem. Chem. Phys.*, 2021, **23**, 16635.

38 J. Kessler, V. Andrushchenko, J. Kapitán and P. Bouř, *Phys. Chem. Chem. Phys.*, 2018, **20**, 4926.

39 T. A. Keiderling, *Chem. Rev.*, 2020, **120**, 3381.

40 G. Shanmugam and P. L. Polavarapu, *J. Am. Chem. Soc.*, 2004, **126**, 10292.

41 Z. Ganim, H. S. Chung, A. W. Smith, L. P. Deflores, K. C. Jones and A. Tokamakoff, *Acc. Chem. Res.*, 2008, **41**, 432.

42 A. Barth, *Biochim. Biophys. Acta*, 2007, **1767**, 1073.

43 Z. Majka, K. Kwiecien and A. Kaczor, *ChemPlusChem*, 2024, e202400091.

44 R. Schweitzer-Stenner, *Phys. Chem. Chem. Phys.*, 2023, **25**, 11908.

45 C. Yuan, S. Li, Q. Zou, Y. Ren and X. Yan, *Phys. Chem. Chem. Phys.*, 2017, **19**, 23614.

46 P. Wormell, P. Michal, A. Scott, K. Venkatesan, K. Mylvaganam, T. V. Arx, J. Kitamura, J. Koshoubu and A. Rodger, *ACS Omega*, 2023, **8**, 37490.

47 A. Rodger, K. Venkatesan, J. R. Aldrich-Wright, C. Brodie and A. E. Garcia-Bennett, *Anal. Chem.*, 2024, **96**, 3810.

48 H. Chi, A. Lakhani, A. Roy, M. Nakaema and T. A. Keiderling, *J. Phys. Chem. B*, 2010, **114**, 12744–12753.

49 H. Torii and H. Sato, *Phys. Chem. Chem. Phys.*, 2018, **20**, 14992.

17922 | *Phys. Chem. Chem. Phys.*, 2024, **26**, 17918–17922

This journal is © the Owner Societies 2024